Nanotechnology **19** (2008) 255501 (7pp) doi:10.1088/0957-4484/19/25/255501

Electrochemical synthesis and characterization of TiO_2 nanoparticles and their use as a platform for flavin adenine dinucleotide immobilization and efficient electrocatalysis

S Ashok Kumar[1], Po-Hsun Lo and Shen-Ming Chen[1]

Department of Chemical Engineering and Biotechnology, National Taipei University of Technology, No. 1, Section 3, Chung-Hsiao East Road, Taipei, 106, Taiwan, Republic of China

E-mail: sakumar80@gmail.com and smchen78@ms15.hinet.net

Received 16 February 2008, in final form 15 April 2008
Published 14 May 2008
Online at stacks.iop.org/Nano/19/255501

Abstract

Here, we report the electrochemical synthesis of TiO_2 nanoparticles (NPs) using the potentiostat method. Synthesized particles have been characterized by using x-ray diffraction (XRD) studies, atomic force microscopy (AFM) and scanning electron microscopy (SEM). The results revealed that the TiO_2 film produced was mainly composed of rutile and that the particles are of a size in the range of 100 ± 50 nm. TiO_2 NPs were used for the modification of a screen printed carbon electrode (SPE). The resulting TiO_2 film coated SPE was used to immobilize flavin adenine dinucleotide (FAD). The flavin enzyme firmly attached onto the metal oxide surface and this modified electrode showed promising electrocatalytic activities towards the reduction of hydrogen peroxide (H_2O_2) in physiological conditions. The electrochemistry of FAD confined in the oxide film was investigated. The immobilized FAD displayed a pair of redox peaks with a formal potential of -0.42 V in pH 7.0 oxygen-free phosphate buffers at a scan rate of 50 mV s^{-1}. The FAD in the nanostructured TiO_2 film retained its bioactivity and exhibited excellent electrocatalytic response to the reduction of H_2O_2, based on which a mediated biosensor for H_2O_2 was achieved. The linear range for the determination of H_2O_2 was from 0.15×10^{-6} to 3.0×10^{-3} M with the detection limit of 0.1×10^{-6} M at a signal-to-noise ratio of 3. The stability and repeatability of the biosensor is also discussed.

(Some figures in this article are in colour only in the electronic version)

1. Introduction

Hydrogen peroxide (H_2O_2) is used as an oxidant, disinfectant and bleaching agent in various industrial and household applications [1–3]. The broad occurrence and application of H_2O_2 therefore require the use of suitable analytical methods for its determination from trace concentration levels up to the levels typically found in food, pharmaceutical, clinical, industrial and environmental samples. H_2O_2 also plays a key role as the product of the enzymatic reaction in coupled enzyme systems [4]. Owing to its importance, several analytical techniques have been employed for its determination, such as titrimetry [5], spectrometry [6], chemiluminescence [7, 8] and electroanalytical methods [9–14]. Among these methods, electroanalytical methods based on the enzyme modified electrodes have several advantages such as low detection limit, less interference, low cost, fast response and being suitable for field analysis.

The flavins are an important class of biochemical compounds which are found in both plants and animals. Due to their importance, most of the flavins have been the subject of

[1] Authors to whom any correspondence should be addressed.

many studies. The flavin containing adenine group is capable of undergoing oxidation–reduction reactions and it can accept either one electron in a two-step process or can accept two electrons at once. In the form of $FADH_2$, it is one of the cofactors that can transfer electrons to the electron transfer chain. FAD is a cofactor in the enzymes D-amino acid oxidase, glucose oxidase, and xanthine oxidase. Trace amounts of FAD play an important role in biological processes, for example, metabolism and normal growth [15–18].

Inorganic n-type semiconductor titanium dioxide (TiO_2) particles have good biocompatibility, stability and environmental safety. Titanium dioxide has been widely used in many areas such as the paint industry, biomedicine, electronics and environmental engineering [19–21]. In recent decades, TiO_2 nanoparticles (NPs) have had direct applications in the preparation of biosensors because of their biocompatibility, large surface area, stability and strong adsorptive ability on various electrode materials [22, 23]. Heme containing proteins such as cytochrome c, myoglobin and hemoglobin have been successfully assembled on TiO_2 NPs, which can keep the natural conformation of the proteins and enhance their electron transfer reactivity [24]. Topoglidis and his co-workers have utilized TiO_2 NPs to immobilize heme proteins to study the adsorption mechanism of the proteins and their interaction with catalytic substrates, as well as to develop a series of biosensors to detect nitric oxide and carbon oxide [25–28]. Zhang *et al* have obtained the direct electron transfer of horseradish peroxidase in TiO_2 NPs and have fabricated a hydrogen peroxide biosensor [29].

In the present paper, we report a disposable amperometric biosensor for the quantification of H_2O_2 in physiological conditions. First, TiO_2 NPs were electrochemically synthesized on an indium tin oxide coated electrode; they were characterized by XRD, AFM and SEM. The TiO_2 NPs were used to modify a screen printed carbon electrode (SPE), and the resulting TiO_2NPs/SPE was used to immobilize FAD enzyme using consecutive cyclic voltammetry (CV). Electrocatalytic reduction reactions of oxygen (O_2) and H_2O_2 were investigated with the FAD and TiO_2 NP modified SPE (FAD/TiO_2NPs/SPE) using CV, rotatable disk electrode (RDE) and amperometry techniques. Thereafter, the FAD/TiO_2NPs/SPE was used as a biosensor for the detection of H_2O_2 in neutral buffer solution.

2. Experimental details

2.1. Materials and apparatus

Flavin adenine dinucleotide disodium salt and titanium oxosulfate $TiOSO_4$ were purchased from Sigma–Aldrich (St. Louis, MO, USA). Hydrogen peroxide (30%, w/w), potassium ferrocyanide, sulfuric acid (H_2SO_4, assay 95%), nitric acid (HNO_3, assay 60%) and sodium hydroxide (NaOH, purity 93%) were purchased from Wako Pure Chemicals (Osaka, Japan). Potassium nitrate, sodium acetate and sodium dihydrogen phosphate (NaH_2PO_4) were obtained from E-Merck (Darmstadt, Germany), and other chemicals were of analytical grade and used without further purification. Double-distilled water was used in all experiments. Diluted H_2O_2 standard solutions were freshly prepared directly prior to use.

Electrochemical measurements were performed with a CHI750A Electrochemical Work Station (CH Instrument Inc., USA). Disposable screen printed carbon electrodes were purchased from Zensor R&D (Taichung, Taiwan) and indium tin oxide (ITO) coated glass electrodes were purchased from Merck Display Technologies, Ltd (Darmstadt, Germany). The ITO thickness and resistance were 30 ± 10 nm and 80 Ω, respectively. The size of the glass was 300 mm × 350 mm × 0.7 mm. The ITO and SPE were used as working electrodes. ITO substrates were cleaned by using detergent, diluted nitric acid and then finally rinsed with distilled water. Platinum wire was used as the counter electrode. All the cell potentials were measured with respect to an Ag/AgCl [KCl (sat)] reference electrode. Hydrodynamic voltammetric studies on the dioxygen reduction reaction and amperometry measurements of H_2O_2 were performed on a Bi-potentiostat Model CHI750A (TX, USA) having an analytical rotator model AFMSRK with MSRX speed control (Rotatable disk electrode PINE Instruments, USA). A model S-3000H scanning electron microscope (Hitachi Scientific Instruments, London, UK) was used for surface image measurements. The AFM images were recorded with a multimode scanning probe microscope system operated in tapping mode using a Being Nano-Instruments CSPM-4000 (Ben Yuan Ltd, Beijing, China). Electrochemical impedance measurements were performed using an impedance measurement unit, IM6ex ZAHNER, Messsysteme (Kroanch, Germany). All experiments were carried out at room temperature.

2.2. Electrochemical synthesis of TiO_2

Cathodic electrosynthesis of TiO_2 NPs was carried out on the ITO electrode from a bath solution containing 0.02 M $TiOSO_4$, 0.03 M H_2O_2, 0.05 M HNO_3 and 0.05–0.25 M KNO_3 (pH 1.4). The deposition was performed at room temperature (25 ± 2 °C) under potentiostatic conditions (−2.0 V versus Ag/AgCl). This led to the formation of a white color gel film on the electrode surface. Each deposition was carried out for 30 min. For the preparation of multiple TiO_2 layers, the electrosynthesis was repeated three or four times, with drying steps at 150 °C in between, after which there was a final annealing step at 400 °C for 1 h to obtain crystalline TiO_2 film. The substrates were weighed prior to coating and after annealing to determine the amount of deposited TiO_2. Nearly 20% mass reduction was observed after heat treatment at 400 °C for 1 h, due to the elimination of water from the film [30]. Thereafter, crystalline TiO_2 particles were scratched from the ITO surface and collected in 10 ml brown colored vial and used later for modification of the SPE. Cathodic electrodeposition of TiO_2 film from $TiOSO_4 + H_2O_2 + HNO_3 + KNO_3$ (pH 1.4) solutions involves the indirect deposition of a gel of hydrous titanium oxo-hydrides (equation (3)), resulting from the reaction of titanium peroxo-sulfate (equation (2)) with the hydroxide ions produced by nitrate electrochemical reduction [31, 32].

$$NO_3^- + H_2O + 2e^- \rightarrow NO_2^- + 2OH^- \quad (1)$$

$$TiOSO_4 + H_2O_2 \rightarrow Ti(O_2)SO_4 + H_2O \quad (2)$$

$$Ti(O_2)SO_4 + 2OH^- + (x+1)H_2O \rightarrow TiO(OH)_2{\cdot}xH_2O_2 + SO_4^{2-}. \quad (3)$$

Annealing of the gel at 400 °C for 1 h results in the formation of crystalline TiO_2 particles (proved by XRD analysis to be rutile).

$$TiO(OH)_2{\cdot}xH_2O \rightarrow TiO_2 + (x+1)H_2O. \quad (4)$$

2.3. Preparation of modified electrodes

5 mg of TiO_2 NPs was added into 10 ml double-distilled water and then ultrasonicated for 10 min to create a suspension with a concentration of 0.5 mg ml^{-1}. After being diluted by five times, 10 μl of TiO_2 NP suspension was spread evenly onto the surface of the SPE, which was then dried for 6 h in the absence of light. Finally, the modified electrode was thoroughly rinsed with double-distilled water. The TiO_2NPs/SPE was cycled in 0.1 M H_2SO_4 solution containing 2×10^{-4} M FAD between the potential ranges of 0.2 to −0.4 V for 40 cycles. Afterward, the electrode was thoroughly rinsed with double-distilled water and then dried at 4 °C for 1 h in the absence of light. When not in use, the electrode was stored in aqueous solution of 0.1 M phosphate buffer solution (pH 7.0) at 4 °C. It is denoted as FAD/TiO_2NPs/SPE, and it was used for further studies. For comparison, a TiO_2NPs coated electrode was prepared and used for further investigation.

3. Results and discussions

3.1. Surface characterizations

AFM (tapping mode) was used to record the topography of the modified electrodes. In this mode, the probe cantilever is oscillated at or near its resonant frequency. The surface morphologies of the TiO_2NPs and FAD/TiO_2NPs coated electrodes exhibit notable features. Figures 1(a) and (b) show 3D AFM images (20 μm × 20 μm) of the TiO_2NPs and FAD/TiO_2NPs films. The average surface roughnesses and peak-to-peak height values are 16, 19 nm and 132, 203 nm for TiO_2NPs and FAD/TiO_2NPs, respectively. The FAD/TiO_2NPs film thickness was 61 nm more than that of the TiO_2NPs film; this difference arose due to the adsorption of FAD films on the oxide surface. The average particle sizes of TiO_2 are found to be in the range of 100 ± 50 nm. Figures 1(c) and (d) show SEM images of the TiO_2NPs and FAD/TiO_2NPs films. The spherical particle aggregates cover the surface (figure 1(c)). The large amount of TiO_2 in the SEM image (figure 1(d)) can be explained by the migration of particles at the surface and adsorption of FAD films on the oxide surface. Figure 2 shows the x-ray diffraction patterns of TiO_2 particles. The experimental spacing were compared with those reported for rutile (110) (2θ of 27.45°) and anatase (101) (25.24°) to identify the particle structure [33]. The XRD results revealed that the synthesized particles are mainly composed of rutile.

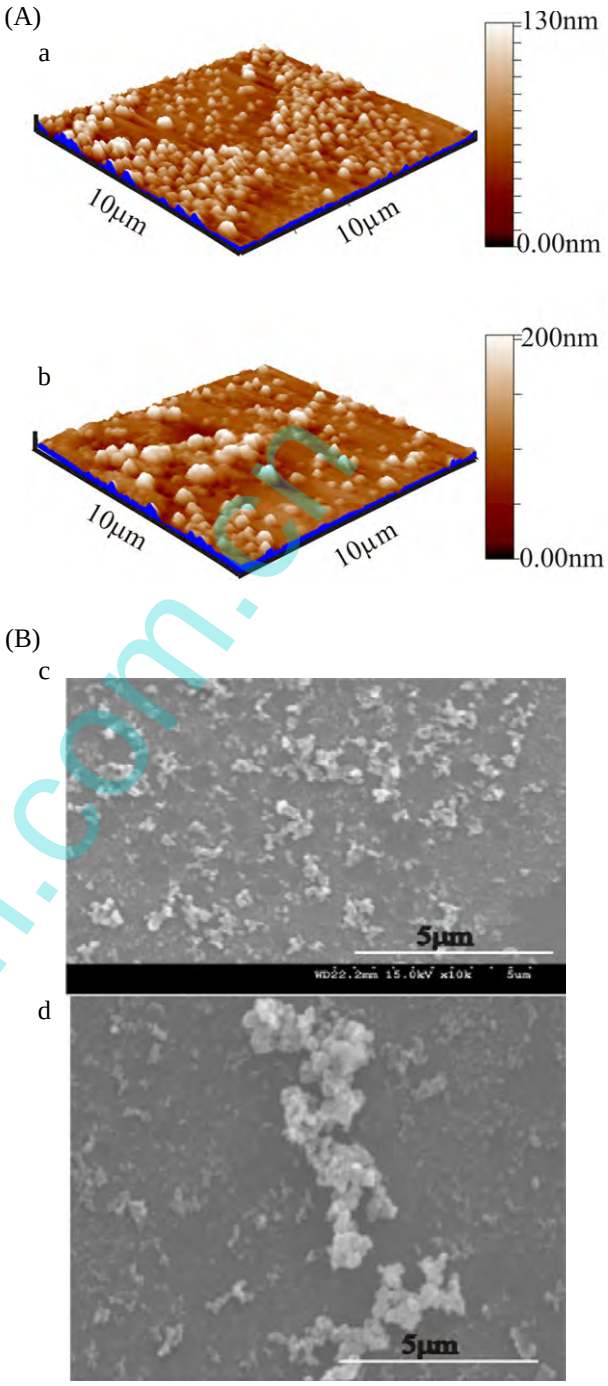

Figure 1. (A) 3D AFM images (20 μm × 20 μm) of (a) TiO_2NPs, and (b) FAD/TiO_2NPs films. (B) SEM images of (c) TiO_2NPs, and (d) FAD/TiO_2NPs films.

3.2. Electrochemical impedance studies

CV and electrochemical impedance spectroscopy (EIS) were used for monitoring each step of SPE modification [34]. The measurements were done in phosphate buffer solution (0.1 M NaH_2PO_4 + 0.1 M KCl; pH 7.0) in the presence of 1 mM $K_3[Fe(CN)_6]/K_4[Fe(CN)_6]$. As expected, $K_3[Fe(CN)_6]/K_4[Fe(CN)_6]$ shows reversible behavior on a bare SPE (figure 3, curve a). After the attachment of TiO_2NPs and FAD, the shape of the cyclic voltammograms changes dramatically. TiO_2NPs and TiO_2NPs/FAD films on the surface of the SPE restrict the electrode conduction (figure 3 curves b and c).

The complex impedance is displayed as the sum of the real (Z_{re}) and imaginary (Z_{im}) components. The bare SPE exhibits

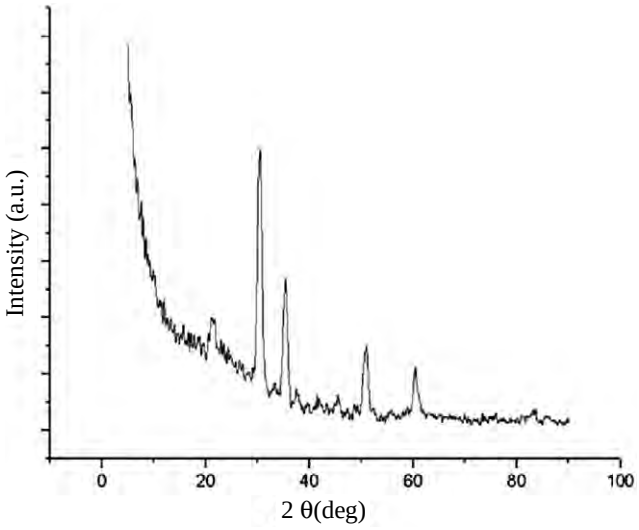

Figure 2. X-ray diffraction patterns of TiO_2 particles.

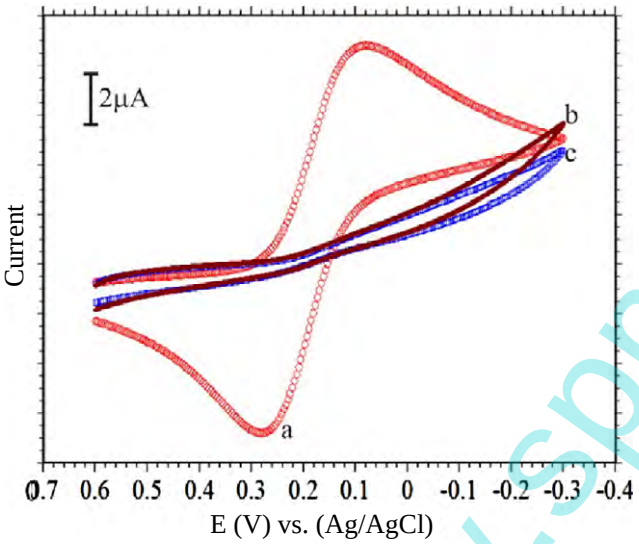

Figure 3. Cyclic voltammograms recorded in 0.1 M PBS containing 1 mM $K_3[Fe(CN)_6]^{3-/4-}$ and 0.1 M KCl: (a) the bare SPE, (b) the TiO_2NPs/SPE, and (c) the FAD/TiO_2NPs/SPE.

almost a straight line of the impedance spectra presented as Nyquist plots (Z_{im} versus Z_{re}), which is characteristic for a limiting step of the electrochemical process (figure 4, curve 1). The semicircle at higher frequencies, which corresponds to the diffusional electron transfer limited process, occurred after the deposition of TiO_2NPs (figure 4, curve 2). This insulating layer on the electrode introduced a barrier to the interfacial electron transfer. The deposition of FAD films on the TiO_2NPs decreased the semicircle diameter, which indicated a lower electron transfer resistance at the electrode interface [35] (figure 4, curve 3). The increase of electron transfer kinetics on the electrode surface originates from the FAD monolayer. The results extracted from EIS measurements (figure 4) connected with each step of the electrode modification are in good agreement with the results obtained from cyclic voltammetry (figure 3). A Randle's equivalent circuit was chosen to fit the

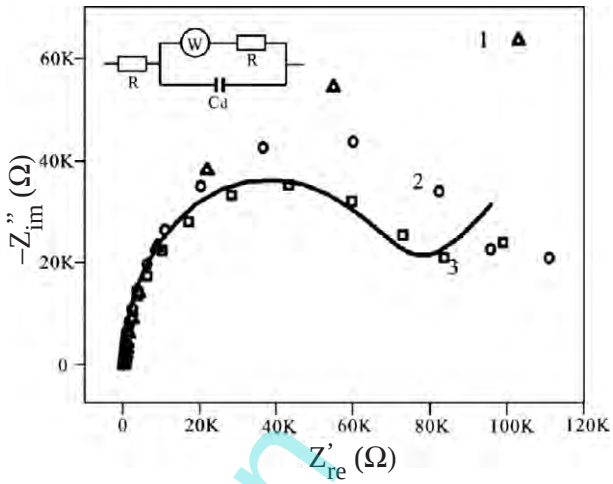

Figure 4. The Nyquist plots for (1) the bare SPE, (2) the TiO_2NPs/SPE and (3) the FAD/TiO_2NPs/SPE in the presence of 1 mM $Fe(CN)_6^{3-}/Fe(CN)_6^{4-}$ by applying an AC voltage with 50 mV amplitude in a frequency range from 100 mHz to 100 KHz. The electrode potential was 0.18 V versus Ag/AgCl. The inset is the Randle's equivalent circuit for FAD/TiO_2NPs/SPE.

obtained impedance data [36]. The circuit model obtained was a good match with experimental results of EIS (figure 4).

3.3. Electrochemical properties

Figure 5 shows the cyclic voltammograms of the FAD/TiO_2 NPs/SPE in acidic solution (pH 1.5) at different scan rates. One reversible redox couple was observed at $E^{0'}$-0.12 V versus Ag/AgCl electrode. Also, the electrochemical response of the FAD/TiO_2NPs/SPE is anticipated for a surface-confined redox couple, because the peak currents were directly proportional to the scan rate up to 200 mV s^{-1} (figure 5), as predicted for a surface-confined process. The ratio of cathodic to anodic peak currents at various scan rates was almost constant. The peak-to-peak potential separation ($\Delta E_p = E_{pa} - E_{pc}$) is about 37 mV for FAD redox peaks at sweep rates below 100 mV s^{-1}, suggesting facile charge transfer kinetics over this range of sweep rate. The surface coverage concentration (Γ) of FAD was evaluated from the following equation:

$$\Gamma = Q/nFA \tag{5}$$

where A (=0.1963 cm^2) is the area of the SPE, n (=2) the number of electrons per reactant molecule, Q the charge obtained by integrating the anodic peak at low voltage scan rate (20 mV s^{-1}), and F is the Faraday constant. We assume that all of the immobilized redox centers are electroactive on the voltammetry timescale. In the present case, the calculated value of Γ was 1.5697×10^{-10} mol cm^{-2}. The formal potential of the FAD redox peak was pH dependent (data not shown). A plot of $E^{0'}$ versus pH gives a straight line from pH 1 to 13 with a slope of −52 mV/pH, which is very close to the anticipated Nernstian value of −59 mV for a two-electron–two-proton process of FAD [37–39] (scheme 1).

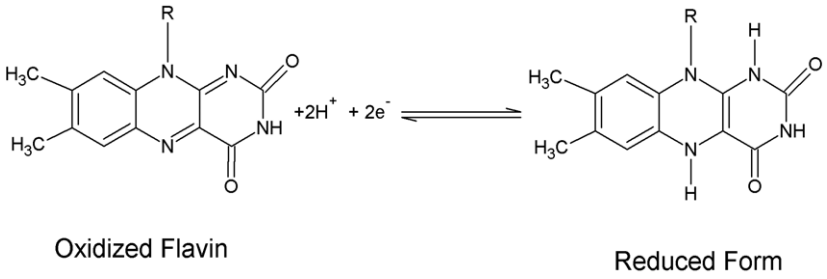

Scheme 1. Redox reactions of FAD.

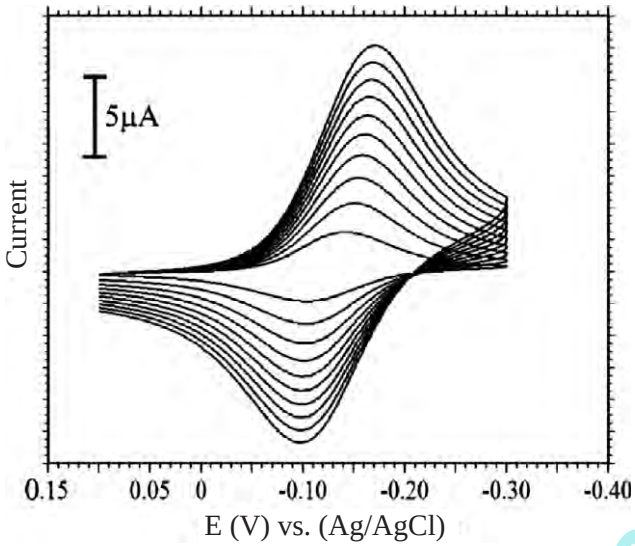

Figure 5. Cyclic voltammograms of the FAD/TiO_2NPs/SPE in 0.1 M H_2SO_4 aqueous solution (pH 1.5) at different scan rates, The scan rates from inner to outer are 0.02, 0.04, 0.06, 0.08, 0.10, 0.12, 0.14, 0.16, 0.18, and 0.20 V s^{-1}, respectively.

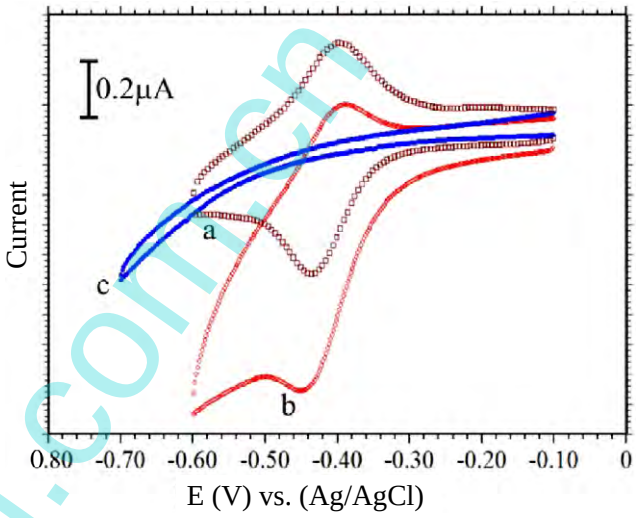

Figure 6. Cyclic voltammograms of the FAD/TiO_2NPs/SPE in pH 7.0 PBS (a) 0.0 mM, (b) 0.15 mM H_2O_2 and (c) bare SPE with 0.15 mM H_2O_2. Scan rate 50 mV s^{-1}.

3.4. Electrocatalysis and amperometric detection of H_2O_2

To investigate the electrocatalytic activity of the FAD/TiO_2 NPs/SPE, electrochemical catalytic reduction H_2O_2 at the FAD/TiO_2NPs/SPE was investigated by CV (figure 6). There was no peak observed at bare the SPE in the presence of H_2O_2 in the potential range of −0.1 to −0.7 V, suggesting that the SPE was inactive to the direct reduction of H_2O_2 (curve c). However, at the FAD/TiO_2NPs/SPE, the reduction peak current at about −0.45 V was greatly enhanced in the presence of H_2O_2 corresponding with the decrease of the oxidation peak current, suggesting a typical electrocatalytic reduction process of H_2O_2. The reduction peak current increased with the concentration of H_2O_2 in the solution (curve b). In the absence of H_2O_2 a reversible redox peak was observed (curve a). The above results indicated that mediated reduction of H_2O_2 takes place at the FAD/TiO_2NPs/SPE, as described in equations (6), and (7).

The amperometric response of the FAD/TiO_2NPs/SPE to successive addition of different concentration of H_2O_2 at the working potential of −0.45 V was also investigated (figure 7). The inset in figure 7 demonstrates the linear relationship of the electrocatalytic current (I_{cat}) versus H_2O_2 concentration in the wide range of 0.15×10^{-6}–3.0×10^{-3} M. The detection limit was found to be 0.1×10^{-6} M ($S/N = 3$) and the sensitivity of the FAD/TiO_2NPs/SPE was 1.86 A M^{-1}.

$$FAD + 2H^+ + 2e^- \leftrightarrow FADH_2 \quad (6)$$

$$FADH_2 + H_2O_2 \rightarrow FAD + 2H_2O. \quad (7)$$

3.5. Electrocatalysis of oxygen

A direct electrocatalytic reduction reaction of O_2 was studied using the FAD/TiO_2NPs/SPE. Figure 8(A) shows the cyclic voltammograms of the FAD/TiO_2NPs/SPE in 0.1 M PBS (pH 7.0) containing O_2 saturated solution. A large increase in the cathodic peak at about −0.48 V is observed in the presence of O_2, and the increase in the cathodic peak is accompanied by a decrease of the anodic peak, suggesting that FAD has mediated the electrocatalytic reduction of O_2 (curve b). The TiO_2NPs/SPE and bare SPE did not shown a significant increase in the peak current and failed to reduce the overpotential required for the O_2 reduction reaction (curves c and d). Indeed, the FAD/TiO_2NPs/SPE reduced the overpotential about 340 mV. In nitrogen saturated solution a reversible redox peak was obtained (curve a).

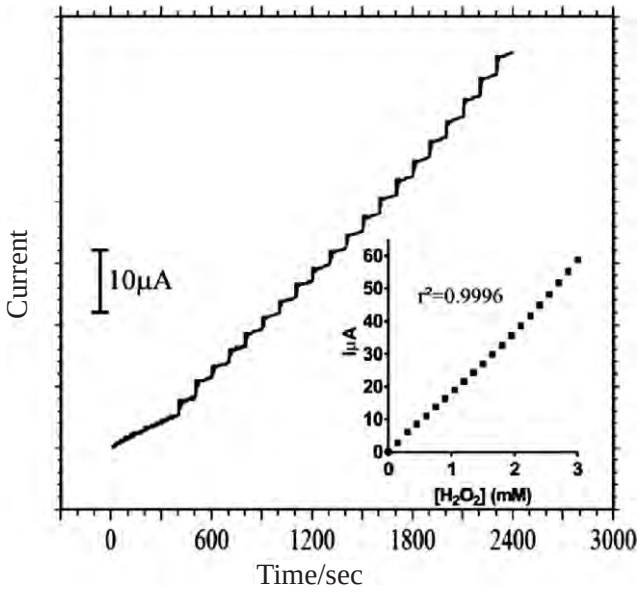

Figure 7. The amperometric responses recorded using the FAD/TiO_2NPs/SPE at an applied potential of −0.45 V versus Ag/AgCl to successive addition of 0.15 mM H_2O_2 in 0.1 M PBS (pH 7.0), rotation rate ∼600 rpm. The inset figure shows the calibration plot.

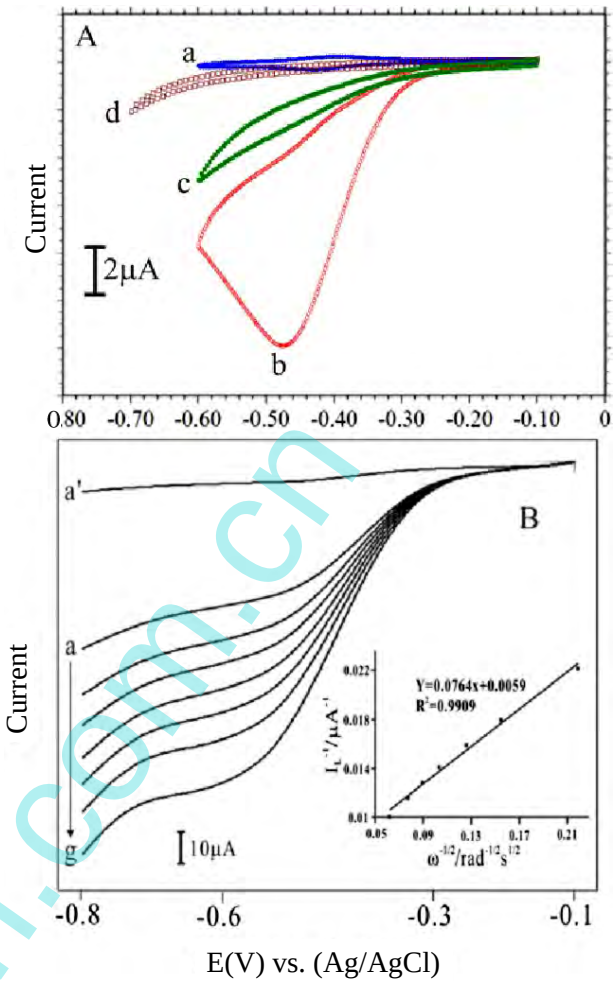

Figure 8. (A) Cyclic voltammograms of the FAD/TiO_2NPs/SPE in pH 7.0 PBS (a) N_2 saturated solution, (b) O_2 saturated solution, (c) TiO_2NPs/SPE with O_2 saturated solution, and (d) bare SPE with O_2. Scan rate 50 mV s^{-1}. (B) Current–potential curves for the reduction of oxygen (saturated) at a rotating glassy carbon disk electrode modified with FAD/TiO_2NPs in pH 7.0 solution at various rotation rates: (a) 200, (b) 400, (c) 600, (d) 900, (e) 1200, (f) 1600 and (g) 2500 rpm (scan rate of 15 mV s^{-1}). The inset figure shows Koutecky–Levich plots.

Figure 8(B) represents a set of current–potential curves in an O_2 saturated buffer solution (pH 7.0) at various angular velocities, ω, with a rotating glassy carbon disk electrode modified with FAD/TiO_2NPs. Curve (a′) is the response of the modified electrode in the absence of oxygen. The limiting current, I_l, is defined as the difference between the currents on a modified electrode at the potential corresponding to the diffusion plateau in deaerated and O_2 saturated solutions. The Levich and Koutecky–Levich plots are formulated from the limiting currents measured at a potential −600 mV and are given in the inset of figure 8(B). The Levich plot in figure 8(B) is very close to the theoretically calculated line for a two-electron process ($n = 2$) and exhibits a linear relationship between limiting current and rotation rate (ω) values. The corresponding Koutecky–Levich plot (figure 8(B)) also shows a linear relationship between I^{-1} and ω^{-1}, with a slope close to that of the theoretical line for the two-electron reduction reaction of oxygen [36, 40]. These findings suggested that the FAD/TiO_2NPs modified glassy carbon disk electrode sustains the reduction of oxygen to H_2O_2 (equations (8)).

$$FADH_2 + O_2 \rightarrow FAD + H_2O_2. \quad (8)$$

3.6. Reproducibility and stability of the modified electrode

The reproducibility of the current response of the biosensor was examined by measuring the H_2O_2 concentration of 1.5 mM, and the relative standard deviation was 2.5 ($n = 9$). It was indicated that the biosensor possessed good reproducibility. In addition, the catalytic current response for reduction of H_2O_2 at the FAD/TiO_2NPs/SPE was tested in the solution containing 1.5 mM H_2O_2 before and after continuously stirring the buffer solution for 30 min. The response of the electrode signal had no significant change before and after stirring the solution; this test indicated that reproducible results can be obtained at the FAD/TiO_2NPs/SPE. After those experiments, the sensor was kept in 0.1 M PBS at 4 °C in order to maintain the activity of FAD. We used the biosensor to detect H_2O_2 three times every day, and the results showed that the catalytic current only decreased about 3.0% after a month. The above results indicated that the FAD/TiO_2NPs/SPE has good stability and that the irreversible adsorption of FAD that occurred onto the TiO_2 films may be due to the interaction between the phosphate moiety of FAD and the TiO_2 layer [41, 42]. According to the earlier reports, phosphate groups have more affinity towards TiO_2 particles; this was confirmed by UV–visible spectra and electrochemical studies [38, 43]. The phosphate groups of FAD may interact strongly with TiO_2 films. Since the electrode preparation is simple, it can be easily prepared and is suitable for commercial purpose.

Table 1. H_2O_2 determination in commercial samples.

Samples	Labeled (%)	Found[a] (%)	RSD (%)	Recovery (%)
A	∼3	2.950	3.36	98.33
B	∼3	2.952	2.91	98.40

[a] Average value of five measurements.

3.7. Determination of H_2O_2 in real samples

To examine the real application of this modified electrode, measurements of H_2O_2 in commercially available antiseptic solutions (sample A) and soft contact lens cleaning solutions (sample B) (∼3% H_2O_2) were analyzed. The commercial solutions were diluted 200 times in phosphate buffer solution; the diluted samples were analyzed with the FAD/TiO_2NPs/SPE using a chronoamperometric method. The results obtained are presented in table 1. In our experiments, the concentration of H_2O_2 was calculated using the standard additions method. The relative standard deviation of each sample for five successive detections is less than 3.36%. In addition, the recovery ratio on the basis of this method was investigated, and the value is between 98.40 and 98.33%. The recovered ratio indicates that the determination of H_2O_2 using the FAD/TiO_2NPs/SPE is effective and can be applied for the detection of H_2O_2 in real samples.

4. Conclusions

The electrochemical synthesis of TiO_2 NPs and their applications as a platform for FAD immobilization have been studied. The FAD/TiO_2NPs/SPE shows excellent stability and electrocatalytic activity towards the reduction of H_2O_2 and O_2 in physiological conditions. AFM, SEM and x-ray diffraction analyses revealed that the TiO_2NPs have covered the electrode surface, leading to the adsorption of FAD films. The electrocatalytic properties of the modified electrode were studied by using cyclic voltammetry, amperometry and RDE methods. The FAD/TiO_2NPs/SPE has been employed as a biosensor for the determination of H_2O_2 in the range from 0.15×10^{-6} to 3.0×10^{-3} M with a detection limit of 0.1×10^{-6} M ($S/N = 3$).

Acknowledgment

This project work was financially supported by the Ministry of Education and the National Science Council of Taiwan (ROC).

References

[1] Watt B E, Proudfoot A T and Vale J A 2004 *Toxicol. Rev.* **23** 51–7
[2] Harms D, Than R, Pinkernell U, Schmidt M, Krebs B and Karst U 1998 *Analyst* **123** 2323–7
[3] Li Y 1996 *Food Chem. Toxicol.* **34** 887–904
[4] Ruzgas T, Csoregi E, Emneus J, Gorton L and Marko-Varga G 1996 *Anal. Chim. Acta* **330** 123–38
[5] Hurdis E C and Romeyn H J 1954 *Anal. Chem.* **26** 320–5
[6] Matsubara C, Kawamoto N and Takamura K 1992 *Analyst* **117** 1781–4
[7] Aizawa M, Ikariyama Y and Kuno H 1984 *Anal. Lett.* **17** 555–64
[8] Nakashima K, Maki K, Kawaguchi S, Akiyama S, Tsukamoto Y and Imai K 1991 *Anal. Sci.* **7** 709
[9] Wang J, Gu M, Di J, Gao Y, Wu Y and Tu Y 2007 *Bioprocess. Biosyst. Eng.* **30** 289–96
[10] Kumar S A and Chen S M 2007 *Biosens. Bioelectron.* **22** 3042–50
[11] Zhu X, Yuri I, Gan X, Suzuki I and Li G 2007 *Biosens. Bioelectron.* **22** 1600–4
[12] Cao S, Yuan R, Chai Y, Zhang L, Li X and Gao F 2007 *Bioprocess. Biosyst. Eng.* **30** 71–8
[13] Salimi A, Sharifi E, Noorbakhsh A and Soltanian S 2007 *Biophys. Chem.* **125** 540–8
[14] Kumar S A and Chen S M 2007 *J. Mol. Catal. A: Chem.* **278** 244–50
[15] Underwood A L and Burnett R W 1973 *Electroanalytical Chemistry* ed A J Bard (New York: Dekker) p 60
[16] Kamal M M, Elzanowska H, Gaur M, Kim D and Birss V I 1991 *J. Electroanal. Chem.* **318** 349–61
[17] Kumar S A and Chen S M 2007 *Sensors Actuators* B **123** 964–77
[18] Kumar S A and Chen S M 2007 *J. Solid State Electrochem.* **11** 993–1006
[19] Turkoglu M and Yener S 1997 *Int. J. Cosmet. Sci.* **19** 193–201
[20] Meacock G, Taylor K D A, Knowles M and Himonides A 1997 *J. Sci. Food Agric.* **73** 221–5
[21] Van der Molen R, Hurksx H, Out-Luiting C, Spies F, van't Noordende J, Koerten H and Mommaas A 1998 *J. Photochem. Photobiol.* B **44** 143–50
[22] Topoglidis E, Discher B M, Moser C C, Dutton P L and Durrant J R 2003 *ChemBioChem* **4** 1332–9
[23] McKenzie K J, Marken F and Opallo M 2005 *Bioelectrochemistry* **66** 41–7
[24] Li Q W, Luo G A and Feng J 2001 *Electroanalysis* **13** 359–63
[25] Topoglidis E, Cass A E G, Gilardi G, Sadeghi S, Beaumont N and Durrant J R 1998 *Anal. Chem.* **70** 5111–3
[26] Topoglidis E, Campbell C J, Cass A E G and Durrant J R 2001 *Langmuir* **17** 7899–906
[27] Topoglidis E, Cass A E G, O'Regan B and Durrant J R 2001 *J. Electroanal. Chem.* **517** 20–7
[28] Topoglidis E, Astuti Y, Duriaux F, Gratzel M and Durrant J R 2003 *Langmuir* **19** 6894–900
[29] Zhang Y, He P L and Hu N F 2004 *Electrochim. Acta* **49** 1981–8
[30] Georgieva J, Armyanov S, Valova E, Poulios I and Sotiropoulos S 2006 *Electrochim. Acta* **51** 2076–87
[31] Karuppuchamy S, Amalnerkar D P, Yamaguchi K, Yoshida T, Sugiura T and Minoura H 2001 *Chem. Lett.* **143** 78
[32] Karuppuchamy S, Nonomura K, Yoshida T, Sugiura T and Minoura H 2002 *Solid State Ion.* **151** 19
[33] Kim S H, Kwak S Y, Sohn B H and Park T H 2003 *J. Membr. Sci.* **211** 157–65
[34] Patolsky F, Zayats M, Katz E and Willner I 1999 *Anal. Chem.* **71** 3171–80
[35] Pei R J, Cheng Z L, Wang E K and Yang X R 2001 *Biosens. Bioelectron.* **16** 355–61
[36] Bard A J and Faulkner L R 1980 *Electroanalytical Methods: Fundamentals and Applications* (New York: Wiley)
[37] Kubota L T, Gorton L, Lanzilotta A R and McQuillan A J 1998 *Bioelectrochem. Bioenerg.* **47** 39–46
[38] Yamashita M, Rosatto S S and Kubota L 2002 *J. Braz. Chem. Soc.* **13** 635–41
[39] Garjonyte R, Malinauskas A and Gorton L 2003 *Bioelectrochemistry* **61** 39–49
[40] Golabi S and Raoof J B 1996 *J. Electroanal. Chem.* **416** 75–82
[41] Ronson T K and McQuillan A J 2002 *Langmuir* **18** 5019–22
[42] Connor P A and McQuillan A J 1999 *Langmuir* **15** 2916–21
[43] Kubota L T, Munteanu F, Roddick-Lanzilotta A, McQuillan A J and Gorton L 2000 *Quim. Anal.* **19** 15–27